

Highly Carbonylated Cellulose Nanofibrous Membranes Utilizing Maleic Anhydride Grafting for Efficient Lysozyme Adsorption

Juncheng Ma,^{†,||} Xueqin Wang,^{‡,||} Qiuxia Fu,[†] Yang Si,[‡] Jianyong Yu,[§] and Bin Ding^{*,†,‡,§}

[†]Key Laboratory of Textile Science & Technology, Ministry of Education, College of Textiles, Donghua University, Shanghai 201620, China

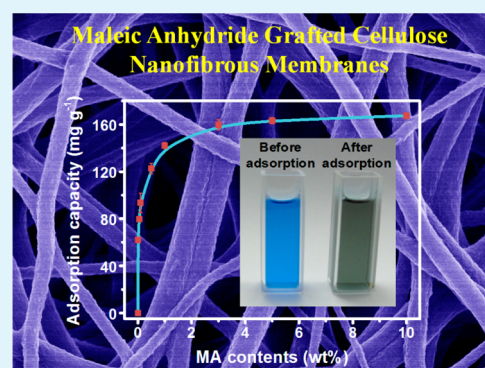
[‡]State Key Laboratory for Modification of Chemical Fibers and Polymer Materials, College of Materials Science and Engineering, Donghua University, Shanghai 201620, China

[§]Nanomaterials Research Center, Modern Textile Institute, Donghua University, Shanghai 200051, China

Supporting Information

ABSTRACT: Construction of adsorptive materials for simple, efficient, and high-throughput adsorption of proteins is critical to meet the great demands of highly purified proteins in biotechnological and biopharmaceutical industry; however, it has proven extremely challenging. Here, we report a cost-effective strategy to create carbonyl groups surface-functionalized nanofibrous membranes under mild conditions for positively charged protein adsorption. Our approach allows maleic anhydride to *in situ* graft on cellulose nanofibrous membranes (CMA) to construct adsorptive membranes with large surface area and tortuous porous structure. Thereby, the resultant CMA membranes exhibited high adsorption capacity of 160 mg g⁻¹, fast equilibrium within 12 h, and good reversibility to lysozyme. Moreover, the dynamic adsorption was performed under low pressure-drops (750 Pa), with a relatively high saturation adsorption amount of 118 mg g⁻¹, which matched well with the requirements for proteins purification. Considering the excellent adsorption performance of the as-prepared adsorptive membranes, this simple and intriguing approach may pave a way for the design and development of robust and cost-effective adsorption membranes to meet the great demands for fast and efficient adsorption of positively charged proteins.

KEYWORDS: electrospun cellulose nanofibrous membranes, maleic anhydride, surface functionalization, lysozyme, adsorption



1. INTRODUCTION

Highly purified proteins play critical roles in biotechnological and biopharmaceutical industry and are in great demand because of their wide range of applications involving immunodiagnosics, immunotherapy, scientific research, food-stuffs, and cosmetics.^{1–4} Conventional methods such as fixed-bed liquid chromatograph, packed beds of porous resins, and pore-size-dependent encapsulation platforms have been used to selectively adsorb and elute the target protein molecules in many biotherapeutics purification processes.^{5–7} Although these approaches possess high binding capacity toward ligands and proteins, they generally suffer from the relatively slow adsorption kinetics, high operation pressure-drops, being time-consuming, and the usage of large quantities of solvents due to the slow intraparticle diffusion of the protein molecules to access the available binding sites in the porous resin beads. Alternatively, fibrous membranes adsorption/chromatography, which is known to possess porous structure, has been successfully applied to purify proteins with lower operation pressure-drops, faster adsorption equilibrium, ease in packing and scale-up, and reduced solvent use.⁸ Unfortunately, the small surface area available for ligands binding and the low

porosity of the currently used membranes led to the limited adsorption capacity and unexpected rapid breakthrough. An efficient way to address this problem is by performing the adsorption process using nanofiber membrane as the platform, since nanofiber membrane is a highly desirable scaffold for immobilization of ligands and capturing proteins owing to its large surface area that enables higher interaction, increases immobilization efficiency, and enhances the long-term stability and reusability.^{9,10} Therefore, utilizing nanofibrous membranes to create adsorptive fibrous membranes has been suggested as a potential alternative approach to achieve promising protein adsorption performance.

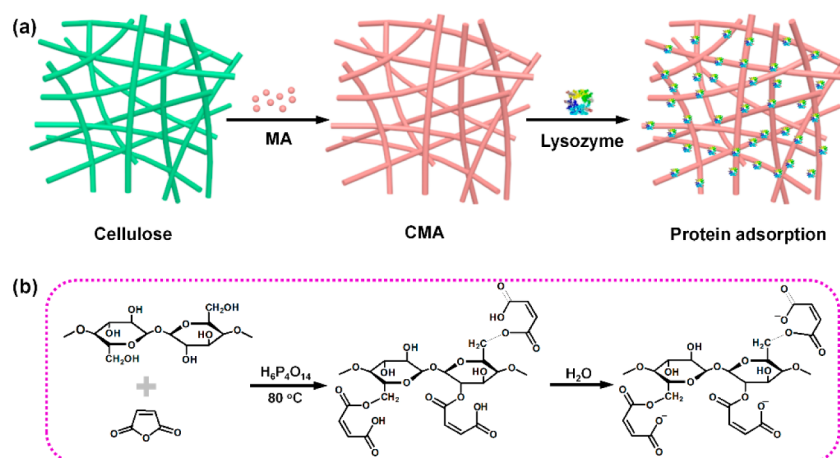
Electrospun nanofibrous membranes as the forefront of advanced fibrous materials, possessing large surface area to volume ratio, high tortuous porous structure, robust mechanical strength, reliability and amenability to large-scale production, and versatility in terms of surface functionalization, have held great promise for constructing functionalized nanofibrous

Received: May 30, 2015

Accepted: July 1, 2015

Published: July 1, 2015

Scheme 1. Schematic Illustration for (a) the Preparation of CMA Nanofibrous Membranes and the Lysozyme Adsorption Process and (b) the Graft Reactions between Cellulose and MA



membranes for application foreground in various fields such as adsorption, filtration, sensing, and oil spill cleanup.^{11–15} Compared with the membranes operating purely on a sieving mechanism, extensive efforts have been devoted to use nanofibrous membranes to adsorb proteins based on dye-ligands interaction, ion exchange, and hydrophobicity due to the outstanding selectivity and reduced pressure-drops. For instance, researchers have developed various adsorptive membranes to selectively purify a variety of proteins such as Cibacron blue F3GA functionalized poly(ether sulfone) membranes,¹⁶ concentrated nitric acid and surfactant treated carbon nanofibers,¹⁷ and poly(isobutylene-*b*-styrene) membranes.¹⁸ The major problems associated with current electrospun nanofibrous membrane-based protein adsorption materials are the expensive dye ligands, extreme modification conditions, and relatively low adsorption capacity, which have restricted their wide applications. The challenge therefore remains in harvesting specific cost-effective nanofibrous membranes with large surface area capable of efficient adsorption of proteins under mild conditions.

In this work, we present an intriguing and economic approach for the construction of carbonyl groups surface-functionalized cellulose nanofibrous membranes under mild conditions for protein adsorption. Previously, carbonyl groups were modified onto the surface by atom transfer radical polymerization, air plasma pretreatment, and concentrated acid treatment,¹⁷ which are inconvenient to process, time-consuming, and hard for large-scale fabrication. Herein, the adsorptive nanofibrous membranes were facile fabricated by first *in situ* immobilization of the maleic anhydride (MA) on the surface of cellulose nanofibers and the subsequent heat treatment (80 °C) to graft MA molecules on cellulose (Scheme 1). To the best of our knowledge, there has been no reported work on employing MA-functionalized materials for proteins adsorption. We demonstrate that our MA-modified cellulose (CMA) nanofibrous membranes exhibit good adsorption performance, involving high lysozyme adsorption capacity, fast adsorption equilibrium, efficient separation performance, and good reversibility. Additionally, considering the adsorbed positively charged proteins on the surface could be eluted by regulating the pH value or the ionic strength of the elution buffer, consequently, the specified proteins could be separated from the mixture of the positively charged proteins; thus, the as-prepared CMA nanofibrous membranes could potentially be

truly applied for protein adsorption. We believe that these membranes made in the investigation could serve as the adsorptive membranes to prepare fibrous membranes adsorption/chromatography for fast and efficient adsorption of positively charged proteins.

2. EXPERIMENTAL SECTION

2.1. Materials and Reagents. Cellulose acetate (CA; $M_w = 30000$; acetyl content of 39.8%) was provided by Sigma-Aldrich Inc., St. Louis, MO, USA. MA and polyphosphoric acid (PPA) were purchased from Aladdin Reagent Co., Ltd., Shanghai, China. *N,N*-Dimethylacetamide (DMAc), acetone, sodium chloride (NaCl), and sodium hydroxide were obtained from Shanghai Chemical Reagent Co., Ltd., China. Lysozyme powder from chicken egg white and bovine serum albumin (BSA) were obtained from Sangon Biotech Co., Ltd., Shanghai, China. Ultrapure water with a resistance of 18.2 M Ω was purified by using a Heal-Force system. The chemicals/materials were all analytical grade and were used as received without further purification.

2.2. Fabrication of Cellulose Nanofibrous Membranes. The cellulose nanofibrous membranes were prepared by hydrolyzing the electrospun CA nanofibrous membranes according to the previous work.¹⁹ Typically, a 15 wt % CA precursor solution was prepared by dissolving CA powder in the mixture solvent of DMAc and acetone (1/2, w/w) and vigorously stirring for 12 h. Afterward, the precursor solution was loaded into syringes with a 5-G metal needle to perform the electrospinning process by using DXES-1 spinning equipment (Shanghai Oriental Flying Nanotechnology Co. Ltd., China). During the process, a high voltage of 25 kV and a controllable feed rate of 0.5 mL h⁻¹ were applied. The resultant nanofibrous membranes were deposited onto the paper-covered grounded rotating roller with a rotation rate of 50 rpm at a 15 cm spinneret-to-collector distance. The relevant temperature and humidity during electrospinning were kept at 25 \pm 2 °C and 45 \pm 5%, respectively. Subsequently, the obtained CA nanofibrous membranes were hydrolyzed in a 0.05 M sodium hydroxide aqueous solution for 7 days at ambient temperature, washed with ultrapure water to neutral, and then dried in the oven to obtain the cellulose nanofibrous membranes.

2.3. Preparation of CMA Nanofibrous Membranes. Typically, a mixture of aqueous solution was first prepared by dissolving a certain amount of MA (0, 0.01, 0.05, 0.1, 0.5, 1, 3, 5, and 10 wt %) in water; simultaneously, the PPA (10 wt % as to MA) was added to the solution to serve as a catalyst, and then the cellulose nanofibrous membranes were immersed in the mixture solution for 10 min to *in situ* immobilize the MA onto the surface of cellulose nanofibers. Subsequently, the membranes were kept in the heating oven at 80 °C for 1 h to undergo the graft reaction to form the CMA nanofibrous membranes. In order to compare the adsorption performance between

nanofibrous membranes and commercial filter paper, the MA-functionalized cellulose filter paper was prepared using the same procedures.

2.4. Testing Adsorption Performance. In this work, lysozyme with the isoelectric point of 10.8 was taken as the positively charged model protein and BSA with an isoelectric point of 4.7 was taken as the negatively charged model protein. Prior to systematically investigation of the adsorption performance, the adsorption toward lysozyme and BSA (at the concentration of 1 mg mL⁻¹) was performed, illustrated in Supporting Information Figure S1. It is clear that the CMA nanofibrous membranes could only adsorb lysozyme ascribed to the electrostatic attraction between the positive charge on the lysozyme and the negative charge on CMA fibers; thus, we investigated the adsorption performance toward lysozyme subsequently. Lysozyme solutions with various concentrations (0.2, 0.4, 0.6, 0.8, 1, 1.2, and 1.5 mg mL⁻¹) and pH values (4, 5, 6, 6.5, 7, and 8) were prepared using phosphate buffer solution. To test the static adsorption performance, 0.5 g of as-prepared CMA nanofibrous membranes was immersed in the lysozyme solution (100 mL) for a certain time, subsequently the absorbance intensity change at 280 nm was detected using an ultraviolet–visible (UV–vis) spectrophotometer, and then the adsorption amount was calculated by using the following equation: $q_e = V(C_0 - C_e)/m$, where q_e is the adsorption amount (mg g⁻¹), V is the volume of the protein solution (mL), C_0 and C_e are the initial and equilibrium concentrations of the protein solution (mg mL⁻¹), and m is the amount of adsorbent (g). According to the Beer–Lambert law, absorbance at the wavelength of 280 nm showed a linear response in all of the concentration range used in the experiments;²⁰ therefore, the C_0 and C_e could be determined based on the absorbance intensity change. Meanwhile, in order to investigate the dynamic adsorption performance, 10 layers of CMA membranes with a diameter of 15 mm and a total thickness of 0.3 mm were sandwiched into a stainless steel filter holder vertically placed on the horizontal position. The freshly prepared lysozyme solution (taking the solution at 1 mg mL⁻¹ as an example) was then poured onto the membranes (flow rate of the 0.2 mL min⁻¹); following interaction with the CMA fibrous membranes, the passed effluent lysozyme solution was collected per 2 mL and set aside for repeated membrane–pass iterations, and then the UV–vis spectra of the collected solution were detected to calculate the adsorption amount. Notably, in the entire process, the operation pressure-drops were kept the same (750 Pa) by controlling the height of the lysozyme solution. Finally, the filter system was rinsed with NaCl solution, and the membranes were extracted and conserved in the buffer.

To investigate the reversible adsorption performance of the as-prepared CMA nanofibrous membranes, the adsorbed fibrous membranes were incubated in the NaCl solution (0.5 M) for 20 min after each cycle to elute the adsorbed lysozyme and then rinsed with ultrapure water for five times to remove the NaCl. Subsequently, the regenerated CMA nanofibrous membranes were immersed into the lysozyme solution to reuse for another cycle.

2.5. Characterization. Field emission scanning electron microscopy (FE-SEM, S-4800, Hitachi Ltd., Tokyo, Japan) was used to examine the morphologies of the fibrous membranes. Fourier transform infrared (FT-IR) spectra were recorded with a Nicolet 8700 FT-IR spectrometer in the range of 400–4000 cm⁻¹. The crystalline structure was characterized by X-ray diffraction (XRD; D/Max-2550 PC, Rigaku Co., Tokyo, Japan). The mechanical properties of the membranes were tested on a tensile tester (XQ-1C, Shanghai New Fiber Instrument Co., Ltd., China) with a crosshead speed of 30 mm min⁻¹. The Brunauer–Emmett–Teller (BET) surface areas of the membranes were characterized by using N₂ adsorption–desorption isotherms with a surface area analyzer (ASAP2020, Micromeritics Co., Norcross, GA, USA). The pore sizes of various membranes were tested by utilizing a capillary flow porometer (CFP-1100AI, Porous Materials Inc., Ithaca, NY, USA). The water contact angle (3 μL) of the nanofibrous membranes was measured by using a contact angle goniometer Kino SL200B. The pH values of the lysozyme solution were measured by using a pH meter (pHs-3c, Shanghai Inesa Scientific Instrument Co., China). The UV–vis spectra were recorded by an

Idea optics PG 2000pro fiber-optic spectrometer (Idea Optics Technology Ltd., Yancheng, China) scanning from 180 to 1180 nm at room temperature.

3. RESULTS AND DISCUSSION

3.1. Morphologies and Structure of Nanofibrous Membranes. The aim of this work is to develop a carboxylic group functionalized nanofibrous membrane for positively charged protein adsorption. Bearing this in mind, we designed the nanofibrous membrane-based protein adsorbents on the basis of three criteria: (1) the adsorbents should have large specific surface area and high porosity; (2) they should have a fully carboxylation functionalized surface to interface with biological systems, and the structure of the nanofibrous membranes should be maintained without obvious change during carboxylation and adsorption process; (3) the nanofibrous membranes should be carboxylated under mild conditions. The first two criteria were satisfied by selecting the electrospun cellulose nanofibrous membranes as platform, because of the large surface area and excellent stability of cellulose nanofibers. It is worth noting that another interesting feature of cellulose—relatively low nonspecific binding—would dramatically enhance the accuracy of the analysis of adsorption performance.²¹ The third criterion was satisfied by combining the cellulose nanofibers with suitable anhydrides (such as MA), which could react at relatively milder conditions compared with carboxylic acid or concentrated mineral acid (such as HNO₃ and H₂SO₄), to yield carboxylic groups functionalized nanofibrous membranes.²²

The representative FE-SEM image of CA nanofibrous membranes shown in Figure 1a illustrated that the fibrous

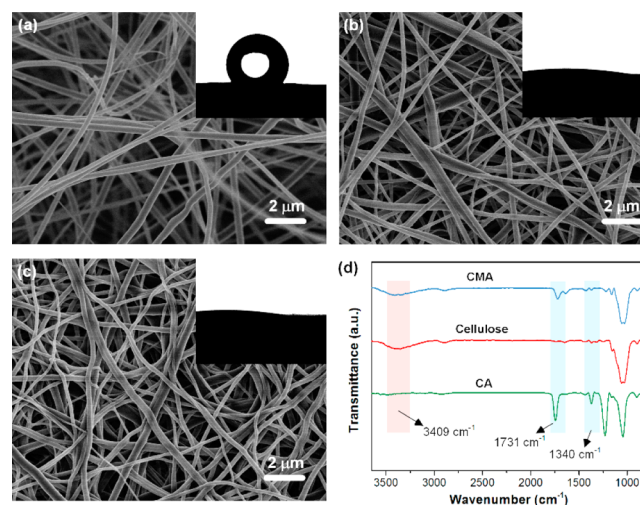


Figure 1. FE-SEM images of (a) CA, (b) cellulose, and (c) CMA nanofibrous membranes. (d) FT-IR spectra of various nanofibrous membranes. The insets are the water contact angles of the corresponding nanofibrous membranes.

membranes were randomly oriented three-dimensional non-woven membranes with an average diameter of 248 nm.^{23,24} Zooming in the FE-SEM image of cellulose nanofibrous membranes, obvious adhesion could be observed and the diameter increased to 267 nm, indicating the accomplishment of the hydrolysis of CA nanofibers.²⁵ XRD analysis (Supporting Information Figure S2) also confirmed that the amorphous CA nanofibers were transferred to cellulose nanofibers with a

crystal form of cellulose II with relevant peaks at 2θ values of 12.4° (110), 20.5° (110), 22.0° (020), which are consistent with the XRD data.²⁶ After heating at 80°C for 1 h, the adhesion structure was significantly enhanced while the diameter (272 nm) negligibly changed, revealing that the MA has firmly adsorbed on the surface of the cellulose nanofibers and the reaction between the -OH groups in cellulose molecules and anhydrides groups in MA have successfully taken place with the help of PPA as a catalyst. Evidence for the hydrolysis of CA nanofibers and the formation of ester on cellulose nanofibers also came from FT-IR spectral analysis (Figure 1d); the characteristic peaks around 3409 cm^{-1} belonged to the stretching vibration of -OH, the peaks around 1731 and 1340 cm^{-1} assigned to C=O and C-O-C stretching vibration of the ester, respectively.²⁷ It is clear that the OH peak appeared after hydrolysis and peak intensity decreased upon reaction with MA, which was in good agreement with the chemical structures of CA, cellulose, and CMA presented in Supporting Information Figure S3. Notably, the hydrophobic CA nanofibrous membranes with a water contact angle of 124° transferred to superhydrophilic cellulose nanofibrous membranes after hydrolysis, and remained superhydrophilic upon reaction with MA, which was consistent with the aforementioned results. Furthermore, the tensile strength of the nanofibrous membranes (Supporting Information Figure S4) enhanced from 1.75 to 10.3 MPa after the hydrolysis and graft polymerization, which could provide benefits for the follow-up dynamic and reversible adsorption process.

The fascinating hierarchical fiber morphologies enabled us to intensively investigate the porous structure of nanofibrous membranes. The relevant N_2 adsorption-desorption isotherm curves displayed in Figure 2a exhibited isotherms of type IV with a H3 hysteresis loop, demonstrating the typical characteristics of mesopores within the as-prepared membranes.^{28,29} Brunauer-Emmett-Teller (BET) surface area analysis showed that CA, cellulose, and CMA nanofibrous membranes possessed similar surface areas of 3.67, 3.49, and 3.28 g m^{-2} , respectively, which were significantly superior to those of commercial fibrous substrates.²² The pore size of the relevant CA nanofibrous membranes (Figure 2b) revealed that the pore-size distribution in the range of 1.2–2.5 μm with a well-developed peak centered at 1.67 μm . After hydrolysis, the average pore size decreased to 0.93 μm ascribed to the adhesion structure, and subsequently decreased to 0.65 μm due to the enhanced adhesion structure in nanofibrous membranes. The tortuous porous structure in nanofibrous membranes could provide numerous microporous channels that could significantly lead to the increments of the active sites for ligands and protein adsorption. The aforementioned results also revealed that the structure of the fibrous membranes was maintained without dramatic change, and the large surface area and the porous structure could provide a large quantity of active sites available for ligand and protein binding. Therefore, the resultant nanofibrous membranes may be suitable for applications in practical proteins purification.

3.2. Effect of MA Contents on Adsorption Performance. Ascribing to the adsorption driven force the electrostatic attraction between the negatively charged group on CMA and protein molecules, the carbonyl group contents of CMA nanofibrous membranes were of great importance to protein adsorption performance; therefore, the effect of MA contents on adsorption capacity was intensively investigated. FT-IR spectra (Supporting Information Figure S5) revealed that the

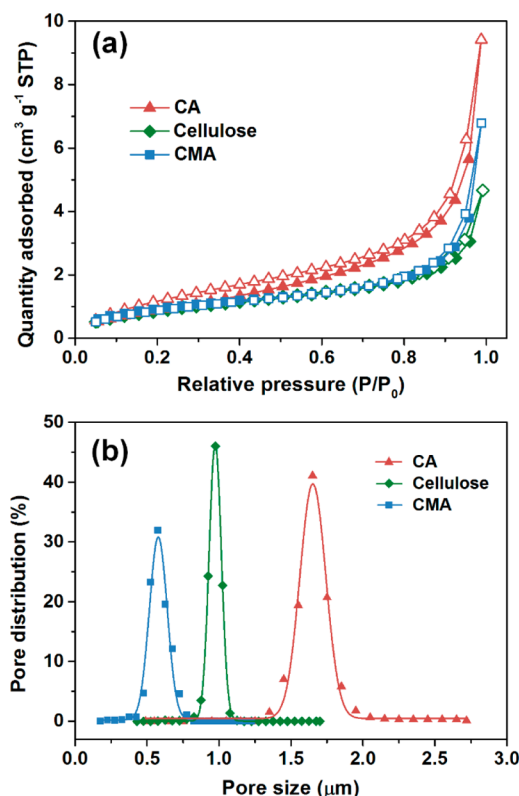


Figure 2. (a) The N_2 adsorption-desorption isotherms of CA, cellulose, and CMA nanofibrous membranes. (b) Pore-size distribution of the various nanofibrous membranes.

peak intensity at 1730 cm^{-1} obviously increased with the increment of the MA contents in solution. Notably, we observed that adding 3 wt % MA could guarantee the carbonyl group on cellulose membranes saturation since further increasing the MA contents could not lead to dramatically intensity change. Fantastically, the maximum adsorption amount of CMA nanofibrous membranes (3 wt % MA) toward lysozyme reached 160 mg g^{-1} , which was obvious higher compared with the MA-functionalized commercial regenerated cellulose filter paper (with a adsorption capacity of 17 mg g^{-1} , shown in Supporting Information Figure S6) and previously reported nanofibrous membranes treated by other methods.³⁰ This is ascribed to the fact that the large surface area of the cellulose nanofibrous membranes provide numerous external binding sites for MA molecules to immobilization; thus, the resultant functionalized nanofibrous membranes possessed numerous active sites for lysozyme adsorption. Additionally, the numerous tortuous microchannels in nanofibrous membranes would provide extra chances for lysozyme adsorption,³¹ thus resulting in the high adsorption capacity toward lysozyme. Furthermore, we used the coomassie brilliant blue G-250 (with brown color) to dye the protein in solution to straightforward display the concentration change of lysozyme solution before and after adsorption using CMA nanofibrous membranes.³² It can be clearly seen that the lysozyme solution initially presented brilliant blue and the color changed to cyan after adsorption by CMA nanofibrous membranes due to the decrease of lysozyme concentration, further demonstrating the conspicuous decrease of lysozyme concentration in solution, as visually shown in the inset of Figure 3.

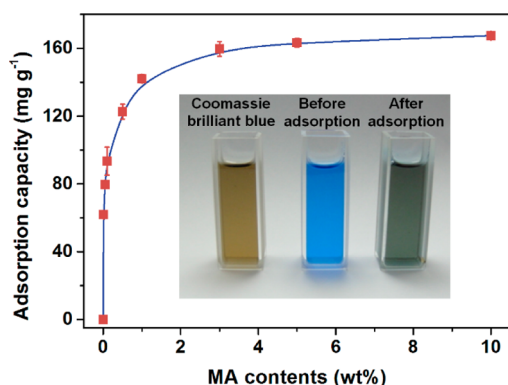


Figure 3. Adsorption performance of CMA nanofibrous membranes with MA at various concentrations. The insets are the optical images of coomassie brilliant blue, solution before and after adsorbing lysozyme using CMA nanofibrous membranes.

3.3. Optimization of Adsorption Conditions. In order to achieve the optimistic protein adsorption performance, the effect of adsorption conditions such as adsorption time, pH values, and initial concentration of lysozyme on adsorption performance have been intensively examined.

The kinetic adsorption performance was first studied by detecting the adsorption amount of CMA nanofibrous membranes at certain time intervals, as shown in Figure 4. It

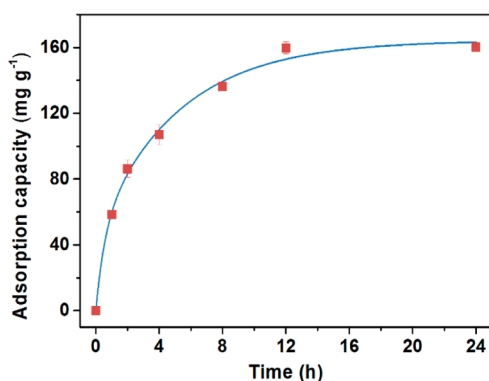


Figure 4. Kinetic adsorption performance of CMA nanofibrous membranes with 3 wt % MA as a function of time.

can be seen that the adsorption capacity increased rapidly with prolonging the adsorption time and reached equilibrium within 8 h, whereas over 12 h of contacting time was required for the adsorption amount value to reach the plateau, indicating the high adsorbing efficiency of lysozyme molecules on CMA nanofibrous membranes. Significantly, the pseudo-first-order and pseudo-second-order models were then used to analyze the adsorption kinetics:^{33,34}

pseudo-first-order kinetics:

$$C = C_0 e^{-k_1 t}, \quad q_t = q_e (1 - e^{-k_1 t})$$

pseudo-second-order kinetics:

$$1/C - 1/C_0 = k_2 t, \quad q_t = q_e^2 k_2 t / (1 + q_e k_2 t), \quad k_2 = (m/V)k_1$$

where C is the concentration of lysozyme at equilibrium, C_0 is the initial concentration of lysozyme, k_1 and k_2 are the rate constants, t is the adsorption time, q_t is the amounts of lysozyme adsorbed at a given time, q_e is the amount of protein

adsorbed at equilibrium, m is the amount of the CMA nanofibrous membranes, and V is the volume of the lysozyme solution. The calculated results (Table 1) confirmed that the

Table 1. Estimated Kinetic Parameters of the Adsorption Isotherm

kinetic models	q_e (mg g ⁻¹)	k	R^2
pseudo-first-order kinetics	200	0.194	0.950
pseudo-second-order kinetics	200	1.548	0.975

pseudo-second-order model was more suitable for describing the adsorption data as attested by the higher correlation coefficient (R^2) compared to the first-order kinetics, implying that the rate-limiting step might be chemisorption.³³ Overall, taking advantage of the numerous external active binding sites which are available for protein immobilization, the as-prepared CMA nanofibrous membranes achieved a much faster adsorption kinetic compared with the adsorptive nanofibrous membranes reported in the literature.^{17,35,36} Conspicuously, the fast adsorption equilibrium endows the CMA nanofibrous membranes with great potential to constitute a membrane adsorption/chromatography for practical purification of proteins in the future.

Lysozyme is positively charged below their isoelectric points (10.8); because the carbonyl groups on CMA fibrous membranes are negatively charged, therefore the as-prepared membranes could adsorb lysozyme relying on their mutual electrostatic attraction.³⁰ Considering that the electrostatic attraction is related to the intensity of the positive charge, the pH value of the lysozyme is crucial for testing the lysozyme adsorption capacity. It could be seen from Figure 5a that the resultant CMA nanofibrous membranes possessed similar

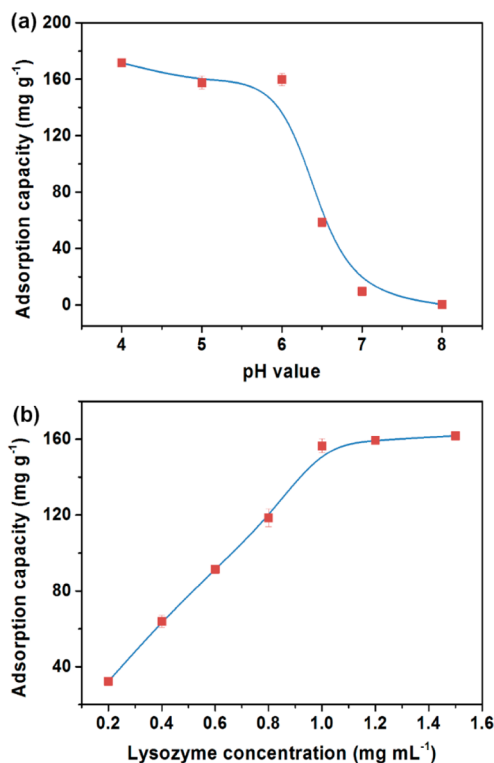


Figure 5. Effect of (a) pH value and (b) initial concentration of lysozyme on the adsorption performance.

adsorption capacities (157–171 mg g⁻¹) when the pH value was lower than 6, while significantly lower adsorption capacities were obtained when the pH value was higher than 6 (0–59 mg g⁻¹). Somewhat unexpectedly, these results are incompatible with previous studies that reported that the optimized pH value for protein adsorption is near to the isoelectric points.³⁷ This phenomenon can be understood considering the fact that the electrostatic attraction between lysozyme and CMA nanofibrous membranes enhanced with the pH value decreased since the proton density increased; consequently, the adsorption rate and capacity increased.³⁸ However, the adsorption capacity would be negligibly changed until the carbonyl groups on CMA nanofibrous membranes have captured a certain amount of proteins and reached the adsorption equilibrium. Consideration of the protein solution with pH value close to neutral is safer and more suitable for practical use; thus the pH value of 6 was selected to perform the follow-up experiments.

Meanwhile, the initial concentration of lysozyme was another important factor dramatically affecting the adsorption capacity,^{39,40} thus the static adsorption isotherms toward lysozyme at different concentration varying from 0.2 to 1.5 mg mL⁻¹ were tested. Figure 5b showed that the adsorption capacity was approximately linear with the lysozyme concentration when the initial concentration was lower than 1 mg mL⁻¹ and then gradually reached the plateau, suggesting the high adsorption efficiency toward lysozyme and the concentration of lysozyme solution should be selected in the range of 0–1 mg mL⁻¹ to guarantee the accuracy of the adsorption experiment. Notably, there was almost no lysozyme adsorption on the cellulose nanofibrous membranes;²¹ thus, the adsorption of CMA fibrous membranes toward lysozyme is further proven to the specific interaction of the carbonyl groups residues with lysozyme.

To quantitatively analyze the adsorption isotherm, Langmuir and Freundlich models were both used that are expressed as follows, respectively:^{39,41}

Langmuir models:

$$1/q_e = 1/q_{\max} + 1/(q_{\max} K_a C)$$

Freundlich models:

$$\log q_e = (\log C)/n + \log K_F$$

where q_{\max} is the maximum adsorption amount at saturation state, K_a is the association saturation constant, and n and K_F are equilibrium constants. The adsorption isotherm of lysozyme on CMA nanofibrous membranes was constructed by plotting the inverse equilibrium lysozyme adsorption capacity against the inverse equilibrium lysozyme concentration and plotting base 10 logarithm equilibrium lysozyme adsorption capacity against base 10 logarithm equilibrium lysozyme concentration, as shown in Supporting Information Figure S7. From the high correlation coefficient ($R^2 = 0.999$) shown in Table 2, it seems

Table 2. Langmuir and Freundlich Constants and Correlation Coefficients for Lysozyme Adsorption on CMA Nanofibrous Membranes

Langmuir constants			Freundlich constants		
q_{\max} (mg g ⁻¹)	K_a (mL mg ⁻¹)	R^2	K_F	n	R^2
186.164	0.0892	0.999	153.517	1.029	0.996

that Langmuir adsorption model is more suitable to describe the adsorption process, demonstrating the adsorption of lysozyme molecules was monolayer adsorption and the interactions between lysozyme molecules were extremely weak. In addition, K_a was calculated to be 0.089 mL mg⁻¹ based on the curve, confirming the existence of strong electrostatic attractions between carbonyl groups and lysozyme.

3.4. Dynamic Adsorption. The ultimate practical evaluation for the adsorption system is the dynamic breakthrough analysis, which is a combination of the equilibrium binding capacity and adsorption kinetics;⁴² thus the CMA nanofibrous membranes were subjected to a dynamic lysozyme adsorption performance test, as illustrated in Figure 6. In a typical

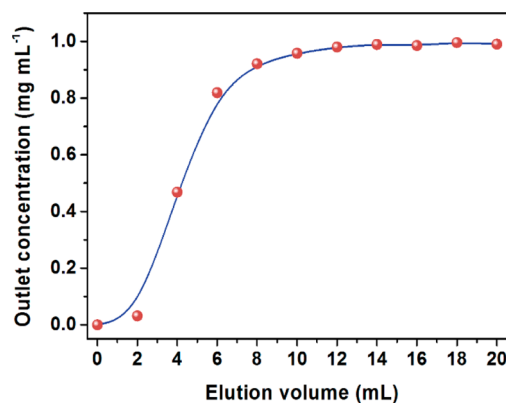


Figure 6. Break-through curve of lysozyme through the CMA nanofibrous membranes (10 layers with a total thickness of 0.3 mm).

adsorption breakthrough curve, the outlet concentration increased slowly and reached the feed concentration until the elution volume accumulated to 12 mL; finally, the saturation dynamic adsorption capacity reached 118 mg mL⁻¹. Considering that the dynamic adsorption was performed under relatively low pressure-drops (750 Pa), such adsorption performance is very promising from the point of view of energy conservation, in contrast to the commercially available regenerated cellulose adsorptive membranes where a driven pressure of more than 10⁵ Pa is usually applied to accomplish the protein purification.^{43,44} Furthermore, it could also be found from the curve that the amount of the desorbed lysozyme was identical with the binding capacity, which means the CMA nanofibrous membranes could also be fully regenerated in the dynamic filter system and is of great importance for real applications

On the other hand, it is known that an ideal adsorptive membrane should possess such effective adsorption performance that the membranes should reach 90% of its saturated adsorption capacity when the outlet concentration reach 10% of the feed concentration.⁴⁵ Nevertheless, the resultant membranes only adsorbed 95.2 mg g⁻¹ protein (80% of the saturation lysozyme adsorption capacity) when the outlet concentration reached 0.5 mg mL⁻¹, which was still less than 90% of the saturation adsorption capacity. Such a broadened breakthrough curve may be ascribed to the fact that the pore size inside the membrane is not uniformly distributed, consequently leading to a broadened mass transfer rate inside the membranes.⁴⁶ In addition, the small membrane total thickness (0.3 mm) of the CMA nanofibrous membranes is another vital factor that significantly decreased the separation efficiency. However, this nonideal separation efficiency of the

CMA nanofibrous membranes does not affect its practical application served as a tool for fast purification of positively charged proteins. To make the as-prepared fibrous membranes suitable for purification process, the structures of the membranes and the process parameters should be further optimized to improve the purification efficiency in future work, involving regulating the porous structure of the membranes by introduction of nanoparticles or a change in the conditions of heat treatment, the total thickness of the nanofibrous membranes, the driven-pressure, and the flow rate of the feeding solution.

3.5. Reversibility of CMA Nanofibrous Membranes.

Generally, it remains an enormous challenge to reserve high adsorption capacity in such adsorption systems after a number of adsorption and regeneration cycles. To achieve a good reversibility, NaCl treatment procedures were introduced to facilitate the regeneration of the CMA fibrous membranes, as shown in Figure 7a. The adsorption capacity of the regenerated

that prevents the CMA nanofibrous membranes from breaking up after repeated use.

4. CONCLUSION

In summary, we have demonstrated a novel strategy for the fabrication of carbonyl group functionalized nanofibrous membranes under mild conditions for lysozyme adsorption. Benefiting from the large surface area to volume ratio, high tortuous porous structure, and the effective carboxylation of the cellulose nanofibrous membranes, the as-prepared CMA nanofibrous membranes possessed high adsorption capacity of 160 mg g^{-1} within 12 h. Moreover, the dynamic adsorption could be performed under low pressure-drops (750 Pa) and the saturation adsorption capacity of the CMA nanofibrous membranes reached 118 mg g^{-1} . Furthermore, the CMA nanofibrous membranes exhibited good reversibility after extended regeneration cycles. Considering the simplicity and cost-effectiveness of the fabrication process, and the excellent adsorption performance including high adsorption capacity, fast adsorption equilibrium, and good reversibility, the CMA nanofibrous membranes provide not only a promising method for purification of lysozyme but also a versatile platform for further development of CMA nanofibrous membrane-based purification systems toward various proteins.

■ ASSOCIATED CONTENT

📄 Supporting Information

Figures showing absorption spectra of the performance of as-prepared CMA membranes and of lysozyme adsorption by utilizing CMA membranes and filter papers, XRD spectra, structures, and tensile stress–strain curves of CA, cellulose, and CMA membranes, FT-IR spectra of CMA nanofibrous membranes with different contents of MA, and the fitting curves of Langmuir and Freundlich isotherm models for lysozyme adsorption on CMA nanofibrous membranes. The Supporting Information is available free of charge on the ACS Publications website at DOI: 10.1021/acsami.5b04741.

■ AUTHOR INFORMATION

Corresponding Author

*E-mail: binding@dhu.edu.cn.

Author Contributions

[†]J.M. and X.W. contributed equally to this work.

Notes

The authors declare no competing financial interest.

■ ACKNOWLEDGMENTS

This work is supported by the National Natural Science Foundation of China (Grant No. 51322304), the Shanghai Committee of Science and Technology (Grant No. 12JC1400101), the Fundamental Research Funds for the Central Universities, and the “DHU Distinguished Young Professor Program”.

■ REFERENCES

- (1) Vohra, A.; Satyanarayana, T. Phytases: Microbial Sources, Production, Purification, and Potential Biotechnological Applications. *Crit. Rev. Biotechnol.* **2003**, *23*, 29–60.
- (2) Johansson, L.; Chen, C. Y.; Thorell, J. O.; Fredriksson, A.; Stone-Elander, S.; Gafvelin, G.; Arner, E. S. J. Exploiting The 21st Amino Acid-Purifying and Labeling Proteins by Selenolate Targeting. *Nat. Methods* **2004**, *1*, 61–66.

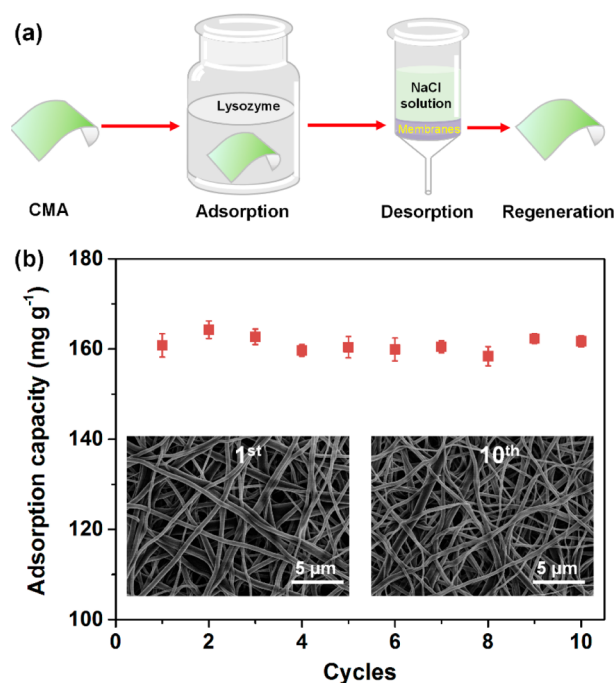


Figure 7. (a) Schematic illustration of the adsorption and regeneration procedures of the as-prepared CMA nanofibrous membranes. (b) Change in the adsorption capacity with increasing cycle number using CMA membranes. The insets are the FE-SEM images of membranes after the first and 10th adsorption/regeneration cycles.

CMA fibrous membranes showed very little difference with that of initial fabricated CMA nanofibrous membranes (Figure 7b), indicating the significant chemical removal of binding proteins and the formation of activated CMA membranes. After 10 regeneration/reuse cycles, the fibrous membranes still exhibited good adsorption performance toward lysozyme and no noticeable difference in structure (insets in Figure 7b) and adsorption capacity could be observed between each of the two cycles. The good reversibility of CMA nanofibrous membranes for lysozyme adsorption mainly ascribes to two contributors: the effective MA surface-functionalized cellulose nanofibrous membranes with no shedding upon regeneration and the robust stability of the unique tortuous interconnected fibrous structure

- (3) Li, Y.; Lin, T. Y.; Luo, Y.; Liu, Q.; Xiao, W.; Guo, W.; Lac, D.; Zhang, H.; Feng, C.; Wachsmann-Hogiu, S.; Walton, J. H.; Cherry, S. R.; Rowland, D. J.; Kukis, D.; Pan, C.; Lam, K. S. A Smart and Versatile Theranostic Nanomedicine Platform Based on Nanoporphyrin. *Nat. Commun.* **2014**, *5*, 4712.
- (4) Li, B.; Jiang, B.; Boyce, B. M.; Lindsey, B. A. Multilayer polypeptide Nanoscale Coatings Incorporating IL-12 for The Prevention of Biomedical Device-Associated Infections. *Biomaterials* **2009**, *30*, 2552–2558.
- (5) Gourdon, P.; Alfredsson, A.; Pedersen, A.; Mahnerberg, E.; Nyblom, M.; Widell, M.; Berntsson, R.; Pinhassi, J.; Braiman, M.; Hansson, O.; Bonander, N.; Karlsson, G.; Neutze, R. Optimized *in Vitro* and *in Vivo* Expression of Proteorhodopsin: A Seven-Transmembrane Proton Pump. *Protein Expression Purif.* **2008**, *58*, 103–113.
- (6) Pai, A.; Gondkar, S.; Sundaram, S.; Lali, A. Expanded Bed Adsorption on Supermacroporous Cross-Linked Cellulose Matrix. *Bioseparation* **1999**, *8*, 131–138.
- (7) Bai, Y.; Glatz, C. E. Capture of A Recombinant Protein from Unclearified Canola Extract Using Streamline Expanded Bed Anion Exchange. *Biotechnol. Bioeng.* **2003**, *81*, 855–864.
- (8) Saxena, A.; Tripathi, B. P.; Kumar, M.; Shahi, V. K. Membrane-based Techniques for The Separation and Purification of proteins: An Overview. *Adv. Colloid Interface Sci.* **2009**, *145*, 1–22.
- (9) Bhattarai, S. R.; Bhattarai, N.; Yi, H. K.; Hwang, P. H.; Cha, D. I.; Kim, H. Y. Novel Biodegradable Electrospun Membrane: Scaffold for Tissue Engineering. *Biomaterials* **2004**, *25*, 2595–2602.
- (10) Erisken, C.; Kalyon, D. M.; Wang, H. Functionally Graded Electrospun Polycaprolactone and Beta-Tricalcium Phosphate Nanocomposites for Tissue Engineering Applications. *Biomaterials* **2008**, *29*, 4065–4073.
- (11) Wang, X.; Ding, B.; Sun, G.; Wang, M.; Yu, J. Electro-Spinning/Netting: A Strategy for The Fabrication of Three-Dimensional Polymer Nano-Fiber/Nets. *Prog. Mater. Sci.* **2013**, *58*, 1173–1243.
- (12) Wang, X.; Si, Y.; Mao, X.; Li, Y.; Yu, J.; Wang, H.; Ding, B. Colorimetric Sensor Strips for Formaldehyde Assay Utilizing Fluoral-p Decorated Polyacrylonitrile Nanofibrous Membranes. *Analyst* **2013**, *138*, 5129–5136.
- (13) Si, Y.; Yu, J.; Tang, X.; Ge, J.; Ding, B. Ultralight Nanofibre-Assembled Cellular Aerogels with Superelasticity and Multifunctionality. *Nat. Commun.* **2014**, *5*, 5802.
- (14) Grafahrend, D.; Heffels, K. H.; Beer, M. V.; Gasteier, P.; Moeller, M.; Boehm, G.; Dalton, P. D.; Groll, J. Degradable Polyester Scaffolds with Controlled Surface Chemistry Combining Minimal Protein Adsorption with Specific Bioactivation. *Nat. Mater.* **2011**, *10*, 67–73.
- (15) Lee, M. W.; An, S.; Latthe, S. S.; Lee, C.; Hong, S.; Yoon, S. S. Electrospun Polystyrene Nanofiber Membrane with Superhydrophobicity and Superoleophilicity for Selective Separation of Water and Low Viscous Oil. *ACS Appl. Mater. Interfaces* **2013**, *5*, 10597–10604.
- (16) Ma, Z.; Lan, Z.; Matsuura, T.; Ramakrishna, S. Electrospun Polyethersulfone Affinity Membrane: Membrane Preparation and Performance Evaluation. *J. Chromatogr. B: Anal. Technol. Biomed. Life Sci.* **2009**, *877*, 3686–3694.
- (17) Schneiderman, S.; Zhang, L.; Fong, H.; Menkhaus, T. J. Surface-Functionalized Electrospun Carbon Nanofiber Mats as An Innovative Type of Protein Adsorption/Purification Medium with High Capacity and High Throughput. *J. Chromatogr. A* **2011**, *1218*, 8989–8995.
- (18) Casiano-Maldonado, M.; Lim, G. T.; Li, X.; Reneker, D. H.; Puskas, J. E.; Wesdemiotis, C. Protein Adsorption on Thermoplastic Elastomeric Surfaces: A Quantitative Mass Spectrometry Study. *Int. J. Mass Spectrom.* **2013**, *354–355*, 391–397.
- (19) Deng, H.; Wang, X.; Liu, P.; Ding, B.; Du, Y.; Li, G.; Hu, X.; Yang, J. Enhanced Bacterial Inhibition Activity of Layer-by-Layer Structured Polysaccharide Film-Coated Cellulose Nanofibrous Mats via Addition of Layered Silicate. *Carbohydr. Polym.* **2011**, *83*, 239–245.
- (20) Yang, Q.; Wu, J.; Li, J. J.; Hu, M. X.; Xu, Z. K. Nanofibrous Sugar Sticks Electrospun from Glycopolymers for Protein Separation via Molecular Recognition. *Macromol. Rapid Commun.* **2006**, *27*, 1942–1948.
- (21) Zhang, L.; Menkhaus, T. J.; Fong, H. Fabrication and Bioseparation Studies of Adsorptive Membranes/Felts Made from Electrospun Cellulose Acetate Nanofibers. *J. Membr. Sci.* **2008**, *319*, 176–184.
- (22) Stenstad, P.; Andresen, M.; Tanem, B. S.; Stenius, P. Chemical Surface Modifications of Microfibrillated Cellulose. *Cellulose* **2008**, *15*, 35–45.
- (23) Ding, B.; Wang, M.; Wang, X.; Yu, J.; Sun, G. Electrospun Nanomaterials for Ultrasensitive Sensors. *Mater. Today* **2010**, *13*, 16–27.
- (24) Si, Y.; Fu, Q. X.; Wang, X. Q.; Zhu, J.; Yu, J. Y.; Sun, G.; Ding, B. Superelastic and Superhydrophobic Nanofiber-Assembled Cellular Aerogels for Effective Separation of Oil/Water Emulsions. *ACS Nano* **2015**, *9*, 3791–3799.
- (25) Wang, X.; Li, Y.; Li, X.; Yu, J.; Al-Deyab, S. S.; Ding, B. Equipment-Free Chromatic Determination of Formaldehyde by Utilizing Pararosaniline-Functionalized Cellulose Nanofibrous Membranes. *Sens. Actuators, B* **2014**, *203*, 333–339.
- (26) Chen, X.; Chen, J.; You, T.; Wang, K.; Xu, F. Effects of Polymorphs on Dissolution of Cellulose in NaOH/Urea Aqueous Solution. *Carbohydr. Polym.* **2015**, *125*, 85–91.
- (27) Morris, N. M.; Catalano, E. A.; Andrews, B. A. K. FT-IR Determination of Degree of Esterification in Polycarboxylic Acid Cross-Link Finishing of Cotton. *Cellulose* **1995**, *2*, 31–39.
- (28) Si, Y.; Tang, X.; Ge, J.; Yang, S.; El-Newehy, M.; Al-Deyab, S. S.; Yu, J.; Ding, B. *In Situ* Synthesis of Flexible Magnetic $\gamma\text{-Fe}_2\text{O}_3\text{/SiO}_2$ Nanofibrous Membranes. *Nanoscale* **2014**, *6*, 2102–2105.
- (29) Si, Y.; Wang, X.; Li, Y.; Chen, K.; Wang, J.; Yu, J.; Wang, H.; Ding, B. Optimized Colorimetric Sensor Strip for Mercury(II) Assay Using Hierarchical Nanostructured Conjugated Polymers. *J. Mater. Chem. A* **2014**, *2*, 645–652.
- (30) Chiu, H. T.; Lin, J. M.; Cheng, T. H.; Chou, S. Y.; Huang, C. C. Direct Purification of Lysozyme from Chicken Egg White Using Weak Acidic Polyacrylonitrile Nanofiber-Based Membranes. *J. Appl. Polym. Sci.* **2012**, *125*, E616–621.
- (31) Menkhaus, T. J.; Varadaraju, H.; Zhang, L.; Schneiderman, S.; Bjostrom, S.; Liu, L.; Fong, H. Electrospun Nanofiber Membranes Surface Functionalized with 3-Dimensional Nanolayers as An Innovative Adsorption Medium with Ultra-High Capacity and Throughput. *Chem. Commun.* **2010**, *46*, 3720–3722.
- (32) Han, X. X.; Xie, Y.; Zhao, B.; Ozaki, Y. Highly Sensitive Protein Concentration Assay over A Wide Range via Surface-Enhanced Raman Scattering of Coomassie Brilliant Blue. *Anal. Chem.* **2010**, *82*, 4325–4328.
- (33) He, X.; Male, K. B.; Nesterenko, P. N.; Brabazon, D.; Paull, B.; Luong, J. H. T. Adsorption and Desorption of Methylene Blue on Porous Carbon Monoliths and Nanocrystalline Cellulose. *ACS Appl. Mater. Interfaces* **2013**, *5*, 8796–8804.
- (34) Azizian, S. Kinetic Models of Sorption: A Theoretical Analysis. *J. Colloid Interface Sci.* **2004**, *276*, 47–52.
- (35) Hardick, O.; Dods, S.; Stevens, B.; Bracewell, D. G. Nanofiber Adsorbents for High Productivity Downstream Processing. *Biotechnol. Bioeng.* **2013**, *110*, 1119–1128.
- (36) Talal, A.; Waheed, N.; Al-Masri, M.; McKay, I. J.; Tanner, K. E.; Hughes, F. J. Absorption and Release of Protein from Hydroxyapatite-Poly(lactic Acid) (HA-PLA) Membranes. *J. Dent.* **2009**, *37*, 820–826.
- (37) Lu, P.; Hsieh, Y. L. Lipase Bound Cellulose Nanofibrous Membrane via Cibacron Blue F3GA Affinity Ligand. *J. Membr. Sci.* **2009**, *330*, 288–296.
- (38) Jones, K. L.; O'Melia, C. R. Protein and Humic Acid Adsorption onto Hydrophilic Membrane Surfaces: Effects of pH and Ionic Strength. *J. Membr. Sci.* **2000**, *165*, 31–46.
- (39) Che, A. F.; Huang, X. J.; Xu, Z. K. Polyacrylonitrile-based Nanofibrous Membrane with Glycosylated Surface for Lectin Affinity Adsorption. *J. Membr. Sci.* **2011**, *366*, 272–7.
- (40) Song, F.; Wang, X. L.; Wang, Y. Z. Fabrication of Novel Thermo-Responsive Electrospun Nanofibrous Mats and Their Application in Bioseparation. *Eur. Polym. J.* **2011**, *47*, 1885–1892.

(41) Tian, P.; Han, X. Y.; Ning, G. L.; Fang, H. X.; Ye, J. W.; Gong, W. T.; Lin, Y. Synthesis of Porous Hierarchical MgO and Its Superb Adsorption Properties. *ACS Appl. Mater. Interfaces* **2013**, *5*, 12411–12418.

(42) Ma, Z.; Masaya, K.; Ramakrishna, S. Immobilization of Cibacron Blue F3GA on Electrospun Polysulphone Ultra-Fine Fiber Surfaces Towards Developing An Affinity Membrane for Albumin Adsorption. *J. Membr. Sci.* **2006**, *282*, 237–244.

(43) Varadaraju, H.; Schneiderman, S.; Zhang, L.; Fong, H.; Menkhaus, T. J. Process and Economic Evaluation for Monoclonal Antibody Purification Using a Membrane-Only Process. *Biotechnol. Prog.* **2011**, *27*, 1297–1305.

(44) Ma, Z. W.; Kotaki, M.; Ramakrishna, S. Surface Modified Nonwoven Polysulphone (PSU) Fiber Mesh by Electrospinning: A Novel Affinity Membrane. *J. Membr. Sci.* **2006**, *272*, 179–187.

(45) Ma, Z. W.; Kotaki, M.; Ramakrishna, S. Electrospun Cellulose Nanofiber As Affinity Membrane. *J. Membr. Sci.* **2005**, *265*, 115–123.

(46) Ma, Z.; Ramakrishna, S. Electrospun Regenerated Cellulose Nanofiber Affinity Membrane Functionalized with Protein A/G for IgG Purification. *J. Membr. Sci.* **2008**, *319*, 23–28.